# Experimental Determination of Dynamic Derivatives in a Wind Tunnel using Parameter Identification

**Thomas Loeser**

DNW-NWB, Lilienthalplatz 7, Braunschweig, Germany

**Detlef Rohlf**

DLR Institute of Flight Systems, Lilienthalplatz 7, Braunschweig, Germany

## *List of Symbols and Abbreviations*

| | |
|---|---|
| b | Wing span; [b] = m |
| $C_L$, $C_D$, $C_Y$ | lift, drag, side force coefficients |
| $C_l$, $C_m$, $C_n$ | rolling, pitching, yawing moment coefficients |
| $c_r$ | Root chord; [$c_r$] = m |
| $f_0$ | Model oscillation frequency; [$f_0$] = Hz |
| p, q, r | Roll rate, pitch rate, yaw rate; [p] = rad/s |
| S | Wing area; [S] = $m^2$ |
| $V_\infty$ | Freestream velocity; [$V_\infty$] = m/s |
| $\alpha$ | Angle of attack, AoA; [$\alpha$] = ° |
| $\beta$ | Angle of sideslip; [$\beta$] = ° |
| $\omega^*$ | Reduced frequency; [$\omega$*] = 1 |

**For the experimental determination of dynamic derivatives a new method is presented. Instead of sinusoidal oscillations the models undergoes specifically designed maneuvers on the wind tunnel's 6 DOF model support. For data evaluation the parameter identification method, as used in flight testing, is employed. The main advantages over the classic approach are significantly reduced testing time and suitability for nonlinear aerodynamic models.**

## *Introduction*

Static or stability derivatives are the rates of change of aerodynamic force and moment coefficients with respect to linear or angular velocity components. Dy-

namic derivatives are the time derivatives thereof. Dynamic derivatives are needed for the determination of stability and control characteristics of new aircraft; they are also required for load assessment of individual airplane components and finally for validation of computational numerical codes.

Dynamic derivatives usually are tested in wind tunnels incorporating special wind tunnel models as well as dedicated test rigs enabling sinusoidal oscillations of the wind tunnel model.

This classic method employs linear models and is for an extended flight envelope not ideally suited as well as rather time consuming. Therefore sinusoidal oscillations have been replaced with suitable manoeuvers in the wind tunnel and System Identification, normally employed for flight tests, has been applied to calculate dynamic derivatives.

## *Test Facility*

### Wind Tunnel

The tests described herein have been performed in the Niedergeschwindigkeits–Windkanal Braunschweig (NWB), belonging to the German–Dutch Wind Tunnels (DNW). The DNW-NWB is an atmospheric low speed wind tunnel which has recently been refurbished to become an aeroacoustic facility. It's main characteristics are a test section size of $3.25 \cdot 2.80$ m$^2$ in either open, slotted or closed configuration. The maximum free stream velocity is $V_\infty = 90$ m/s in the closed test section and $V\infty = 80$ m/s in the open test section. The turbulence intensity in the closed test section is $Tu_x = 0.06$ %; the background noise at $V\infty = 45$ m/s is approximately 60 db(A). Further information about the DNW-NWB can be found in [1], [2] and [3]. A sketch of the wind tunnel is given in **Figure 1**.

### Wind Tunnel Support

The model is mounted by means of a ventral sting on NWB's Model Positioning Mechanism MPM. The MPM can be described as a 6-Degree-of-Freedom (DOF) parallel kinematics system incorporating six struts of constant length whose joints at the wind tunnel fixed side connect to six electric linear motors and on the other side connect to the *Stewart platform*, which thereby obtains three translator and three rotatory degrees of freedom. The electric linear motors traverse along two rails, which are, like the Stewart platform, located above the test section. The MPM is in operation since 2004 and can be employed in combination with the open or closed test section configuration. The MPM can be used for high precision static model positioning as well as for sinusoidal model oscillations and arbitrary pre-defined manoeuvers within its working space.

To augment the working space about model-fixed pitch and roll axes an additional electric actuator is mounted on the Stewart platform, controlled by the same software as the linear motors ("7$^{th}$ axis"). The additional actuator then drives a pushrod; dedicated balance mounts inside the model convert the pushrod motion into the desired model oscillation. The frequency can be set continuously from $f_0 = 0.0$ Hz to $f_0 = 3.0$ Hz. In general, the amplitude range depends on the frequency, the oscillation type and on the balance mount. The development of the dynamic testing systems at DNW-NWB, leading finally to the MPM, is described in [4]. The MPM supporting the DLR-F12 wind tunnel model in NWB's open test section is depicted in **Figure 2**.

**Wind Tunnel Models**

The wind tunnel models used for the dynamic measurements described have been made from carbon fiber composite material in order to keep the model weight as low as possible, therefore reducing inertial forces and moments. The combination of high stiffness and low weight also leads to Eigenmode frequencies, which are in the order of one magnitude above the intended oscillation frequencies. For the wind tunnel tests described in this paper the DLR-F19 model has been employed. The DLR-F19, together with its predecessor, the NASA built SACCON of identical geometry, is a generic UCAV configuration with a 53° leading edge sweep and a lambda wing planform, as shown in **Figures 3** and **4**. The model has a wing span of $b = 1.54$ m, a root chord of $c_r = 1.06$ m and a wing area of $S = 0.77$ m$^2$.

This configuration was established within the NATO/RTO Task group AVT-161 "Assessment of Stability and Control Prediction Methods for NATO Air and Sea Vehicles "[5]. The design and manufacture of the DLR-F19 model as well as the wind tunnel tests at DNW-NWB with the F19 have been performed within the NATO STO AVT-201 Task Group " Extended Assessment of Stability and Control Prediction Methods for NATO Air Vehicles"[6], [7].

## *Data Evaluation*

Data acquisition for all dynamic tests has been performed using a HBM+ data acquisition system with a sampling frequency of $f_s = 600$ Hz for balance and pressure data. There were no corrections for wall or blockage effects applied to the forced motion time history data. The model's attitude was measured with a pair of video cameras, evaluating the location of markers applied to the model surface at a sampling frequency of $f_s = 600$ Hz. The calculation of the derivatives is based on the assumption, that the wind tunnel model is ideally stiff and all tests are performed around symmetrical flow conditions ($\beta_0 = 0°$).

For all further data evaluation the mass and inertial forces, which are always contained in the balance signals recorded in wind-on conditions, when the model

performs an unsteady motion, have to be eliminated. This can be achieved by performing measurements with the model executing exactly the same oscillation (or manoeuver) in wind-off conditions. The subtraction of the Wind-Off data from the Wind-On data is in case of the evaluation by Fourier analysis done after the calculation of the Fourier coefficients (described in [8]); in case of evaluation by Parameter Identification prior to the Identification.

**Classic Approach**

It is assumed that the aerodynamic forces and moments are linear functions of model position and angular speed, or, at heave and lateral oscillation to be linear functions of translatory speed and acceleration. Several methods for calculation of dynamic derivatives, based on a linear assumption, exist [9].

E.g. for a pitching oscillation the Fourier analysis according to [8] yields the following pitching moment derivatives: $C_{m_0}$, $C_{m_\alpha}$ and $C_{m_{\dot{\alpha}}} + C_{m_q}$ and corresponding derivatives for $C_X$ and $C_Z$. In the case of $C_m$ .The result of a linear analysis, taking only the fundamental frequency in account, is given in **Figure 5**, indicating clearly the inadequate representation of nonlinear aerodynamic data.

**Parameter Identification**

General approach

Early in 2009, DLR confirmed the general applicability of its System Identification (SysID) method to dynamic wind tunnel data (**Figure 6**), demonstrating the basic, but limited potential of linear aerodynamic models. The core of the Matlab/Simulink® based SysID procedure[10] is an output error Parameter Identification (PID) algorithm which was in this application used to minimize the difference between model-fixed measured and simulated forces and moments or their coefficients respectively. While the parameters appearing in the aerodynamic model are estimated with a standardized procedure, the model structure must be developed through engineering judgment and reasoning.

In the current SysID step, DLR is developing an equivalent nonlinear aero-model to enable real-time 6-DoF flight mechanical simulations. This implies that the stability parameters can be predicted at intermediate $\alpha$ reference values (& oscillation frequencies). The essential advantages of the 6-DoF approach is the fact that a single set of longitudinal & lateral-directional coefficients/derivatives is covering the entire tested $\alpha$ regime, accounting additionally for aerodynamic cross couplings.

Nonlinear Approach

Whilst the linear approach may give good reliable results for the low $\alpha$ regime where the flow is relatively linear, they are likely to be unsuitable for modeling

the more complex effects of the nonlinear flow at higher α. The nonlinear approach in this paper addresses this by making use of a more general nonlinear model. The model was developed to provide the approximation of the aerodynamic total aircraft coefficients without direct modeling of the vortical airflow characteristics (so called equivalent modeling).

The six equations are based on a number of angle-of-attack breakpoints to cope with the nonlinearities in the angle-of-attack dependencies and uses linear interpolation in between. The breakpoints themselves are estimated along with the aeroparameters so as to be concentrated in the areas with significant changes of the angle-of-attack dependent derivatives. Furthermore, a simple smoothing function is applied to the total coefficients in order to remove excessive peaks, i.e., each data value is adjusted depending on the spacing of the associated angle-of-attack value to the preceding and succeeding angle-of-attack breakpoints. The derivatives are linear with respect to the other input signals which are β, q, r , and angle-of-attack rate, $\dot{\alpha}$ *(the roll rate, p, is not yet used)*. The rates are calculated in a preprocessing step by means of numerical differentiation. In the case of plunge tests, the difference $\dot{\alpha}$ - q is used to avoid high correlations during the estimation of $\dot{\alpha}$ and q derivatives. In all other test cases, the signals of $\dot{\alpha}$ and q are identical.

Drag is modeled as a function of lift to the power of 4 scaled by a 'vortex drag factor', FvD, which is to be estimated. In the longitudinal equations, a traditional high lift hysteresis formula is used in addition, influencing primarily lift, but also drag and pitching moment. Thus, the equivalent aero-model equations are as follows *(clean configuration)*:

$$
\begin{aligned}
CL &= CL0 + CL\alpha + CL\beta + CL(q + \dot{\alpha}) + CLr + CL\dot{\alpha} + CLhys,\\
CD &= CD0 + CD\alpha + CD\beta + CD(q + \dot{\alpha}) + CDr + CD\dot{\alpha} + CDhys + FvD*CL^4,\\
CY &= CY0 + CY\alpha + CY\beta + CY(q + \dot{\alpha}) + CYr + CY\dot{\alpha},\\
Cl &= Cl0 + Cl\alpha + Cl\beta + Cl\ (q + \dot{\alpha}) + Clr + Cl\dot{\alpha},\\
Cm &= Cm0 + Cm\alpha + Cm\beta + Cm(q + \dot{\alpha}) + Cmr + Cm\dot{\alpha} + Cmhys,\\
Cn &= Cn0 + Cn\alpha + Cn\beta + Cn(q + \dot{\alpha}) + Cnr + Cn\dot{\alpha},
\end{aligned}
$$

with *(i = L, D, Y, l, m, n)*:

$$
\begin{aligned}
Ci\alpha &= Ci\alpha\ (Bp) * \alpha(t-\Delta t\alpha),\\
Ci\beta &= [\ Ci\beta\ (Bp) * \alpha(t-\Delta t\alpha)\ ] * \beta(t-\Delta t\beta),\\
Ci(q+\dot{\alpha}) &= [\ Ci(q+\dot{\alpha})\ (Bp) * \alpha(t-\Delta t\alpha)\ ] * q(t-\Delta tq),\\
Cir &= [\ Cir\ (Bp) * \alpha(t-\Delta t\alpha)\ ] * r(t-\Delta tr),\\
Ci\dot{\alpha} &= [\ Ci\dot{\alpha}\ (Bp) * \alpha(t-\Delta t\alpha)\ ] * (\dot{\alpha}\ (t-\Delta t\alpha) - q(t-\Delta tq)).
\end{aligned}
$$

Each of the coefficients consists of a constant part and parameter values at each breakpoint (Bp) which are valid above the corresponding angle-of-attack breakpoint, i.e., each parameter value gives the actual slope relative to the preceding segment. Thus, a total α slope is accumulated to represent a quasi-steady coefficient trajectory (which is - in contrast to linear methods - not the steady-state trajectory, however close to it). The hysteresis loops are then added to this quasi-steady coefficient using equivalent time delays, k(t-Δtk), in α, β, q, r and $\dot{\alpha}$ to roughly approximate the non-stationary changes in the vortex formations.

The traditional high lift hysteresis formula applied for system identification purposes is a hyperbolic function depending on angle-of-attack and is often used

to model the stall characteristics of conventional airplanes due to partial airflow separation (see [11, 12, 13]):

$$XLi = ( 1 - \tanh[ C1*(\alpha(t-\Delta t\alpha) - TAU*\dot{\alpha}\,(t-\Delta t\alpha) - ALsep) ] ) / 2,$$
$$CLhys = CL\alpha*( 1/4*[ 1+\mathrm{sqrt}(XLi) ]^2 -1 ),$$
$$CDhys = CDX*XLi,$$
$$Cmhys = CmX*XLi,$$

with C1, ALsep and TAU, as well as CDX and CmX to be estimated.

Here, C1 characterizes the reduction in slope of the lift curve, ALsep the separation point where half of airflow is detached, and TAU describes the 'breathing' of the hysteresis. CDX and CmX are hysteresis influence factors on drag and pitching moment respectively. For the evaluation of control surface efficiencies, the model equations must extended accordingly using the above described model structure based on the predefined $\alpha$-breakpoints.

**Manoeuver Generation in the Wind Tunnel**

During flight tests, the aircraft motion is induced by control surface deflections which are optimized to excite the aircraft characteristic motions without high correlations in the parameters to be estimated. In the wind tunnel, the excitation of the model motion is performed directly by the MPM using fixed control surface deflections. Apart from sinusoidal oscillations at fixed reference conditions, the MPM can execute arbitrary manoeuvers *(e.g. optimized for parameter identification purposes)*, which have to be defined in tabular form for all axes, trigger and time. The time step doesn't have to be constant but can be – even within one manoeuver definition – adapted to the accelerations, which have to be resolved. The smallest time step is 10 ms. The maximum number of time steps depends on the maneuver definition and is approximately 2000. The input file finally has to be converted to a SINUMERIK-readable program, which then can be executed by the MPM.

For the latest test campaign with the DLR-F19 model, new quasi-steady maneuvers with superimposed harmonic excitations or frequency sweeps (**Figure 7**) were designed to significantly reduce the time for the wind tunnel experiments and to improve the quality of the aerodynamic dataset generation based on nonlinear parameter identification methods. All maneuvers performed are based on a "1 – cosine" $\alpha$-sweep generated by the Stewart platform of the MPM with an amplitude of either $\Delta\alpha = 5°$ or $\Delta\alpha = 10°$, yielding a $\alpha$ range of $\alpha = 0°$ to $\alpha = 10°$ and $\alpha = -6°$ to $\alpha = 14°$ respectively. Superimposed upon this quasi-steady $\alpha$ sweep are harmonic oscillations of either constant or varying frequency. For the SACCON tests the superimposed oscillations have been pitching oscillations with an amplitude of $\Delta\alpha = 4.5°$ and frequencies of 1, 2 or 3 Hz, generated by the 7$^{th}$ axis.

The MPM permits to superimpose motions about other axes, e.g. rolling or yawing oscillations. This has been done during other test campaigns.

**Results**

Parameter Identification Approach

**Figure 8** shows a time histories fit of the DLR-F19 longitudinal and lateral aerodynamic coefficients due to pitch axis excitation, the wind tunnel data in blue and the identification model output in red. The first time slice contains a slow quasi-static pitch maneuver, the second time slice a slow quasi-static pitch maneuver with a superimposed $\alpha$-sweep starting with a slow frequency, and the third time slice a slow quasi-static pitch maneuver with a superimposed $\alpha$-sweep starting with a high frequency. The latter two excitations are combined to induce different frequencies throughout the angle-of-attack regime. The time histories show clearly the nonlinear behavior of the coefficients. Despite of the "noisy" effects at high angle-of-attack, the model fit is very good, simulating the essential nonlinearities. **Figure 9** shows the cross plot fit of the pitching coefficient, in this case of the quasi-static pitch maneuver. In blue again the wind tunnel data, in red the dynamic model output, and in green only the quasi-static portion of the model output without the hysteresis effects due to separation and re-attachment of the airflow *(being intentionally small in this case)*. As in the time histories fit, the essential nonlinear effects are replicated, and the noise level increases with angle-of-attack. **Figure 10** shows the cross plot fit of the pitching coefficient due to the quasi-static pitch maneuvers with superimposed $\alpha$-sweeps. In this case the hysteresis effects due to separation and re-attachment of the airflow are significant, as intended. The green quasi-static portion of the model output is exactly the same as in Figure 9 because all tests were evaluated in a single identification run. Now the hysteresis loops are significant but again quite well reproduced.

## *Conclusion*

The combination of the MPM's dynamic capabilities at DNW-NWB and the System Identification expertise at the DLR Institute of Flight Systems allows the experimental determination of dynamic derivatives in a wind tunnel using Parameter Identification. The main advantages over classical linear evaluation methods are the ability of modeling highly non-linear aerodynamic behavior and a substantially reduced number of wind tunnel measurements in order to generate results for a complete envelope ($\alpha$, $\beta$, eventually deflections of control surfaces). The wind tunnel time saving depends on the test program but can exceed 75%.

## *References*

[1] Bergmann, A.: “The New Aeroacoustic Low Speed Facility DNW-NWB”, AIAA-2012-2173, 18th AIAA/CEAS Aeroacoustics Conference, 4-6 June 2012, Colorado Springs, Colorado, USA

[2] Pott-Pollenske, M.; von Heesen, W. and Bergmann, A.: “Acoustical Preexamination Work and Characterization of the Low Noise Wind Tunnel DNW-NWB”, AIAA-2012-

2175, 18th AIAA/CEAS Aeroacoustics Conference, 4-6 June 2012, Colorado Springs, Colorado, USA
[3] Loeser, T. and Schröder, E.: “The Anechoic Plenum of the DNW-NWB Aeroacoustic Wind Tunnel”, AIAA-2012-2179, 18th AIAA/CEAS Aeroacoustics Conference, 4-6 June 2012, Colorado Springs, Colorado, USA
[4] Bergmann, A.: “Modern Wind Tunnel Techniques for Unsteady Testing – Development of Dynamic Test Rigs”. In: Hermann Schlichting – 100 Years, Springer (2009), pp. 59 - 77
[5] Cummings, R. M. and Schütte, A.: "An Integrated Computational/Experimental Approach to UCAV Stability & Control Estimation: Overview of NATO RTO AVT-161", AIAA-2010-4392, June 2010
[6] Cummings, R. M. and Schütte, A.: "The NATO STO AVT-201 Task Group " Extended Assessment of Stability and Control Prediction Methods for NATO Air Vehicles", AIAA-2014-2394, June 2014
[7] Vicroy, D.., Huber, K.., Rohlf, D. and Loeser, T.: Low-speed Dynamic Wind Tunnel Test Analysis of a Generic 53° Swept UCAV Configuration; AIAA-2014-2003; June 2014
[8] Loeser, T.: Experimental Research of Dynamic Derivatives of Unsteady Moved Aircraft; in ”Experimental Determination of Dynamic Stability Parameters”, VKI LS 2008-02, The von Karman Institute for Fluid Dynamics, Rhode-St-Genèse, Belgium
[9] Rohlf, D.; Schmidt, S. and Irving, J.: "Stability and Control Analysis for an Unmanned Aircraft Configuration Using System-Identification Techniques"; J. Aircraft, Vol. 49, No. 6, Nov-Dec 2012
[10] Seher-Weiß, S., “User's Guide: FITLAB Parameter Estimation Using MATLAB - Version 2.0”, DLR Internal Report, DLR-IB 111-2007/27
[11] Hamel, P. G., and Jategaonkar, R. V., “Evolution of Flight Vehicle System Identification,” Journal of Aircraft, Vol. 33, No. 1, 1996, pp. 9-28
[12] Jategaonkar, R. V., Fischenberg, D., and von Grünhagen, W., “Aerodynamic Modeling and System Identification from Flight Data – Recent Applications at DLR,” Journal of Aircraft, Vol. 41, No. 4, 2004, pp. 681-691
[13] Jategaonkar, R. V., “Flight Vehicle System Identification: A Time Domain Methodology”, Vol. 216, AIAA Progress in Astronautics and Aeronautics Series, Published by AIAA Reston, VA, USA, ISBN 1-56347-836-6, August 2006

## *Figures*

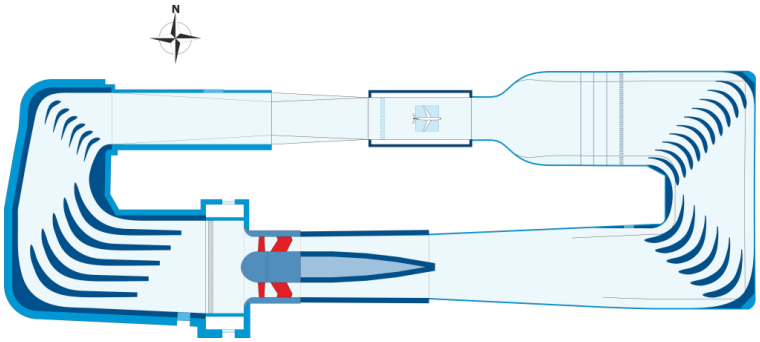


Figure 1: Schematic View of the DNW-NWB

Figure 2: The Model Positioning Mechanism (MPM) in the DNW-NWB, supporting the DLR F12 model

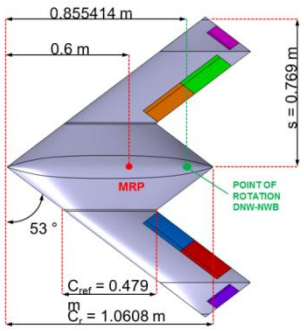


Figure 3: Geometry of the DLR-F19 configuration

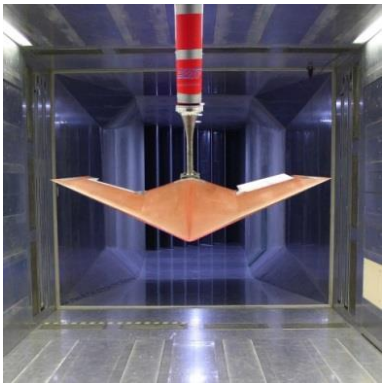

Figure 4: DLR-F19 in the DNW-NWB

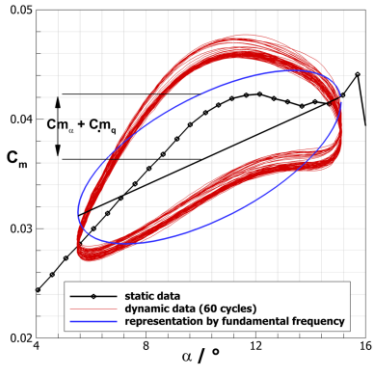


Figure 5:, static and dynamic values of Cm, plus representation of linear analysis

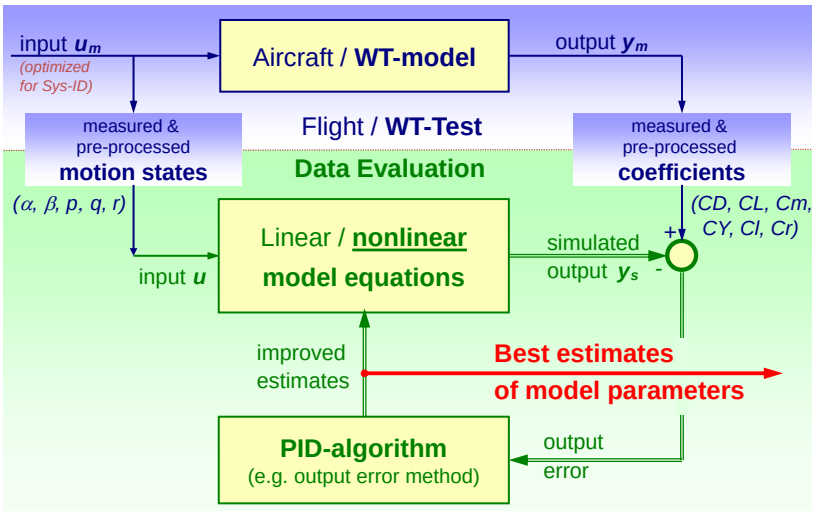


Figure 6: Basic DLR system identification procedure

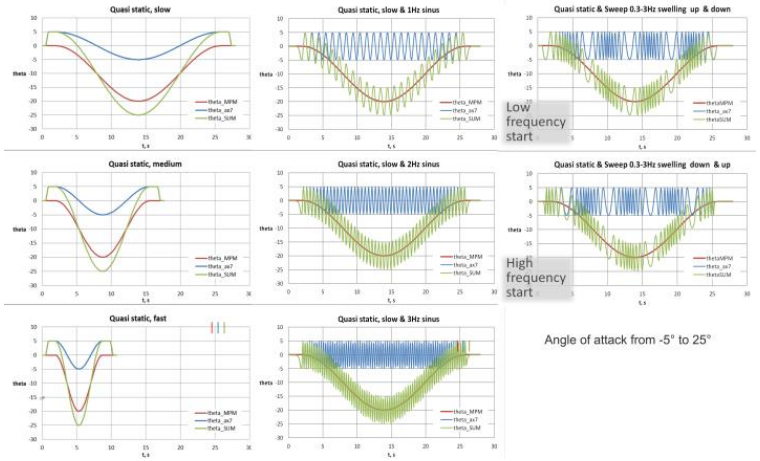


Figure 7: Classes of maneuvers applied for the DLR-F19 configuration

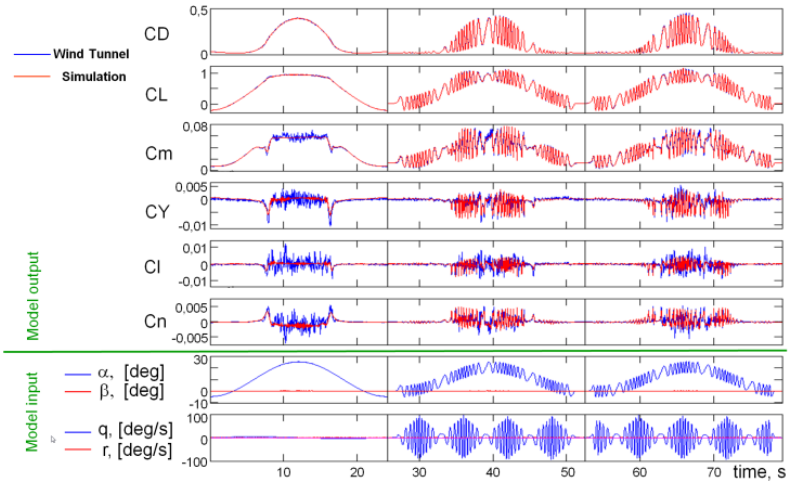


Figure 8: DLR-F19 time histories fit of slow quasi-static excitations and α-sweeps up/down

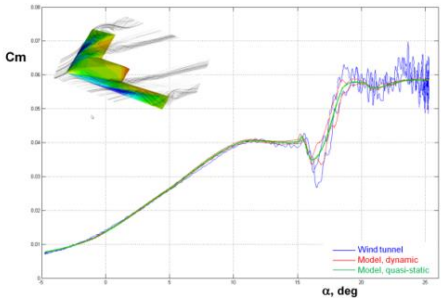


Figure 9: DLR-F19 cross plot fit of pitching moment coefficient, slow quasi-static excitation

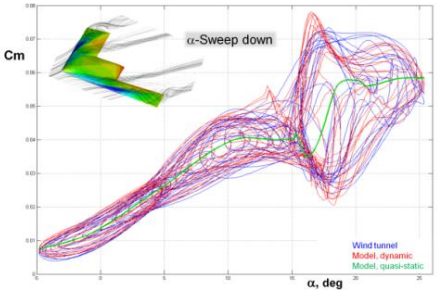


Figure 10: DLR-F19 cross plot fit of pitching moment coefficient, maneuver:α-sweep down